Available online at www.sciencedirect.com
ScienceDirect
Journal of Organometallic Chemistry 692 (2007) 4129–4138
Journal of Organometallic Chemistry
www.elsevier.com/locate/jorganchem

Synthesis and characterization of new Rh^I complexes bearing CO, PPh_3 and chelating *P*,*O*- or *Se*,*Se*-ligands: Application to hydroformylation of styrene

Konstantinos A. Chatziapostolou [a], Kalliopi A. Vallianatou [b], Alexios Grigoropoulos [a], Catherine P. Raptopoulou [c], Aris Terzis [c], Ioannis D. Kostas [b,*], Panayotis Kyritsis [a,*], Georgios Pneumatikakis [a]

[a] *Inorganic Chemistry Laboratory, Department of Chemistry, National and Kapodistrian University of Athens, Panepistimiopolis, Zografou, 15771 Athens, Greece*
[b] *National Hellenic Research Foundation, Institute of Organic and Pharmaceutical Chemistry, Vas. Constantinou 48, 11635 Athens, Greece*
[c] *Institute of Materials Science, NCSR "Demokritos", 153 10 Aghia Paraskevi Attikis, Greece*

Received 3 May 2007; received in revised form 14 June 2007; accepted 19 June 2007
Available online 27 June 2007

Abstract

The complexes [Rh(CO)(PPh_3){$Ph_2PNP(O)Ph_2$-*P*,*O*}] (**3**), [$Rh(CO)_2${$Ph_2P(Se)NP(Se)Ph_2$-*Se*,*Se*′}] (**5**), and [Rh(CO)(PPh_3){$Ph_2P(Se)NP(Se)Ph_2$-*Se*,*Se*′}] (**6**), were synthesised by stepwise reactions of CO and PPh_3 with [Rh(cod){$Ph_2PNP(O)Ph_2$-*P*,*O*}] (**2**) and [Rh(cod){$Ph_2P(Se)NP(Se)Ph_2$-*Se*,*Se*′}] (**4**), respectively. The complexes **3, 5** and **6** have been studied by IR, as well as ^1H and ^{31}P NMR spectroscopy. The *ν*(CO) bands of complexes **3** and **6** appear at approximately 1960 cm^{-1}, indicating high electron density at the Rh^I centre. The structure of complexes **3** and **6** has been determined by X–ray crystallography, and the ^{31}P NMR chemical shifts have been resolved *via* low temperature NMR experiments. Both complexes exhibit square planar geometry around the metal centre, with the five-membered ring of complex **3** being almost planar, and the six-membered ring of complex **6** adopting a slightly distorted boat conformation. The C–O bond of the carbonyl ligand is relatively weak in both complexes, due to strong π-back donation from the electron rich Rh^I centre. The catalytic activity of the complexes **2**, **3** and **6** in the hydroformylation of styrene has been investigated. Complexes **2** and **3** showed satisfactory catalytic properties, whereas complex **6** had effectively no catalytic activity.
© 2007 Elsevier B.V. All rights reserved.

Keywords: *P*,*O*-Ligand; *Se*,*Se*-Ligand; Hemilabile ligand; Rhodium complex; Homogeneous catalysis; Hydroformylation

1. Introduction

Rhodium-based catalyst precursors with phosphorus-containing ligands exhibit remarkable catalytic activity in highly important industrial reactions involving CO insertion to organic substrates, such as hydroformylation of alkenes and carbonylation of methanol [1–4]. In particular, complexes bearing the so-called hemilabile ligands that have at least two different donor-atoms, such as P and E = N, O, S, Se, exhibit interesting coordination chemistry and have been successfully applied to homogeneous catalysis [5,6]. Complexes *cis*-[RhCl(CO){$Ph_2P(CH_2)_nP(O)Ph_2$-*P*,*O*}], $n = 1$, 2, for instance, were shown to be efficient catalyst precursors towards carbonylation of methanol

* Corresponding authors. Tel.: +30 210 7274268; fax: +30 210 7274782 (P. Kyritsis); tel.: +30 210 7273878; fax: +30 210 7273831 (I.D. Kostas).
E-mail addresses: ikostas@eie.gr (I.D. Kostas), kyritsis@chem.uoa.gr (P. Kyritsis).

0022-328X/$ - see front matter © 2007 Elsevier B.V. All rights reserved.
doi:10.1016/j.jorganchem.2007.06.032

at low temperature [7]. Also, the complex *cis*-[RhI(CO){$Ph_2PCH_2P(S)Ph_2$-*P*,*S*}] [8] exhibited better catalytic activity for this reaction compared to the classic Monsanto catalyst $[RhI_2(CO)_2]^-$, under mild conditions. Likewise, in a series of papers, Dutta et al. have explored the efficiency of Rh^I catalyst precursors modified with *P*,*O*- [9] and *P*,*Se*- [10,11] diphosphine ligands, including kinetic studies with respect to oxidative addition reactions on these complexes. In addition, Rh^I complexes with bidentate *P*,*O*-ligands, were shown to catalyze the hydrogenation and the isomerization of 1-hexene, as well as the transfer dehydrogenation of cyclooctane [12]. Trzeciak et al. have investigated Rh^I catalysts modified either with (2-hydroxyphenyl)diphenylphosphine [13] or ferrocene-based *P*,*O*-ligands for the hydroformylation of 1-hexene [14,15].

The results of the above studies demonstrate the ability of mixed donor *P*,*E*-ligands (E = O, S, Se) to regulate the electronic properties of the metal centre in such a way, that an efficient catalyst is produced. The aforementioned complexes show characteristically low *v*(CO) bands, between 1960 cm^{-1} and 1990 cm^{-1} (Table 1). Most probably, the electron-donating *P*,*E*-ligands increase the electron density of the metal centre, thus enhancing π-back-bonding to the π*-orbitals of the CO ligands. In this context, the use of a *Se*,*Se*-bidentate ligand is expected to produce also an electron rich Rh^I centre.

In recent years, we have engaged in preparing several functionalized phosphorus ligands containing additional potent donors such as N, O or S, which were found to lead to improved systems for the rhodium-catalyzed hydroformylation [16–22]. In the work described here, Rh^I–carbonyl complexes with the *P*,*O*-ligand $[Ph_2PNP(O)Ph_2]^-$ [23], or the *Se*,*Se*-ligand $[Ph_2P(Se)NP(Se)Ph_2]^-$ [24], have been explored. These chelating ligands form five- and six-membered rings with the metal centre, respectively. The complexes were structurally and spectroscopically characterized, and shown to contain electron rich Rh^I centres. Thereafter, their catalytic behavior towards hydroformylation of styrene was investigated, in an attempt to elucidate the structural or electronic factors that determine their activity.

Table 1
Comparison of the *v*(CO) in Rh^I complexes with some *P*,*E*-ligands (E = O, S, Se)

Complex	*v*(CO) (cm^{-1})	Reference
cis-[RhCl(CO){$Ph_2P(CH_2)_nP(O)Ph_2$-*P*,*O*}], *n* = 1, 2	1985, 1995	[7]
cis-[RhI(CO){$Ph_2PCH_2P(S)Ph_2$-*P*,*S*}]	1992	[8]
[RhCl(CO){4-$Ph_2PC_6H_4COOMe$-*P*,*O*}]	1977	[9]
[RhCl(CO){$Ph_2PCH_2P(Se)Ph_2$-*P*,*Se*}]	1977	[10]
[RhCl(CO){$Ph_2PN(CH_3)P(Se)Ph_2$-*P*,*Se*}]	1981	[10]
trans-[Rh{dpf-*P*,*O*}(CO)(PPh_3)]	1965	[14]
[Rh{$OC_6H_4PPh_2$-*P*,*O*}(CO)(PPh_3)]	1963	[13]
[Rh(CO)(PPh_3){$Ph_2PNP(O)Ph_2$-*P*,*O*}]	1964	This work
[Rh(CO)(PPh_3){$Ph_2P(Se)NP(Se)Ph_2$-*Se*,*Se*′}]	1962	This work

2. Results and discussion

2.1. Synthesis and spectroscopic characterization of the rhodium complexes

2.1.1. Rh^I complexes with the *P*,*O*-ligand

The synthetic pathway for these complexes is outlined in Scheme 1. Reaction of $[RhCl(cod)_2]_2$ with two equivalents of the ligand $Ph_2PNHP(O)Ph_2$ yields complex [RhCl(cod){$Ph_2PNHP(O)Ph_2$-*P*}] (**1**). Deprotonation of the coordinated *P*,*O*-ligand in **1** by treatment with potassium *tert*-butoxide (^{t}BuOK) yields complex [Rh(cod){$Ph_2PNP(O)Ph_2$-*P*,*O*}] (**2**), according to already reported procedures [23]. The stepwise reaction of **2** with CO and PPh_3, yields the yellow solid [Rh(CO)(PPh_3){$Ph_2PNP(O)Ph_2$-*P*,*O*}] (**3**). The reaction of **2** with CO in a CH_2Cl_2 solution was recorded by IR spectroscopy. The spectrum of the reaction mixture shows two terminal *v*(CO) bands at 2084 cm^{-1} and 1992 cm^{-1}, whereas the (cod) bands are absent, thus confirming the replacement of (cod) by two CO ligands. Subsequent treatment of the Rh–dicarbonyl complex solution with a stoichiometric quantity of PPh_3 afforded complex **3**. The IR spectrum of **3** exhibits a single terminal *v*(CO) band at 1964 cm^{-1}, a value characteristic of an electron rich rhodium centre [3,25]. The shift to lower energy of the *v*(CO) band, compared to the intermediate dicarbonyl complex, indicates a weaker C–O bond due to the enhanced π-back-bonding to the only remaining CO ligand. Other characteristic changes in the IR bands between complexes **1** and **2** have already been reported elsewhere [23]. An overall list of the IR bands of **1**–**3** is presented in Table 2. One can observe the shift to lower energy of the *v*(PO) band going from **1** to **2** due to deprotonation and chelation of the bidentate ligand, the generation of the dicarbonyl complex in solution upon reaction with CO and, finally, the existence of a single *v*(CO) band in **3** after the reaction series is complete. Such Rh^I complexes have been shown to exhibit high catalytic activity towards hydroformylation of olefins [26], or similar catalytic reactions like carbonylation of methanol [11,25].

The three P atoms of **3** are chemically and magnetically non-equivalent (Fig. 1); therefore, the ^{31}P NMR spectrum of **3** exhibits three ddd-peaks (Figs. 2, S1 and S3). The low-field peak ($\delta_P = 80.6$, ddd) is assigned to the P(III) atom ($\mathbf{P}_A$) of the bidentate ligand, which is directly attached to the Rh^I centre and thus deshielded. The $^1J_{RhP}$ coupling constant of 119.0 Hz lies within the typical values of similar systems [12,27,28]. The extremely strong coupling with the P atom of the phosphine ligand ($^2J_{PP} = 327.5$ Hz) can only be rationalized in the context of a *trans* arrangement between $\mathbf{P}_A$ and $\mathbf{P}Ph_3$ [13–15,27–31]. The oxidized P(V) atom ($\mathbf{P}_X$) of the bidentate ligand is not directly coordinated to the metal centre, thus coupling with ^{103}Rh is weak ($^3J_{RhP} = 3.7$ Hz), as expected [23,32,33]. Coupling with $\mathbf{P}_A$($^2J_{PP} = 52.8$) and $\mathbf{P}Ph_3$($^3J_{PP} = 41.3$ Hz) gives rise to a ddd-peak ($\delta_P = 68.9$). The chemical shifts for the two non-equivalent P-atoms of the bidentate *P*,*O*-ligand are

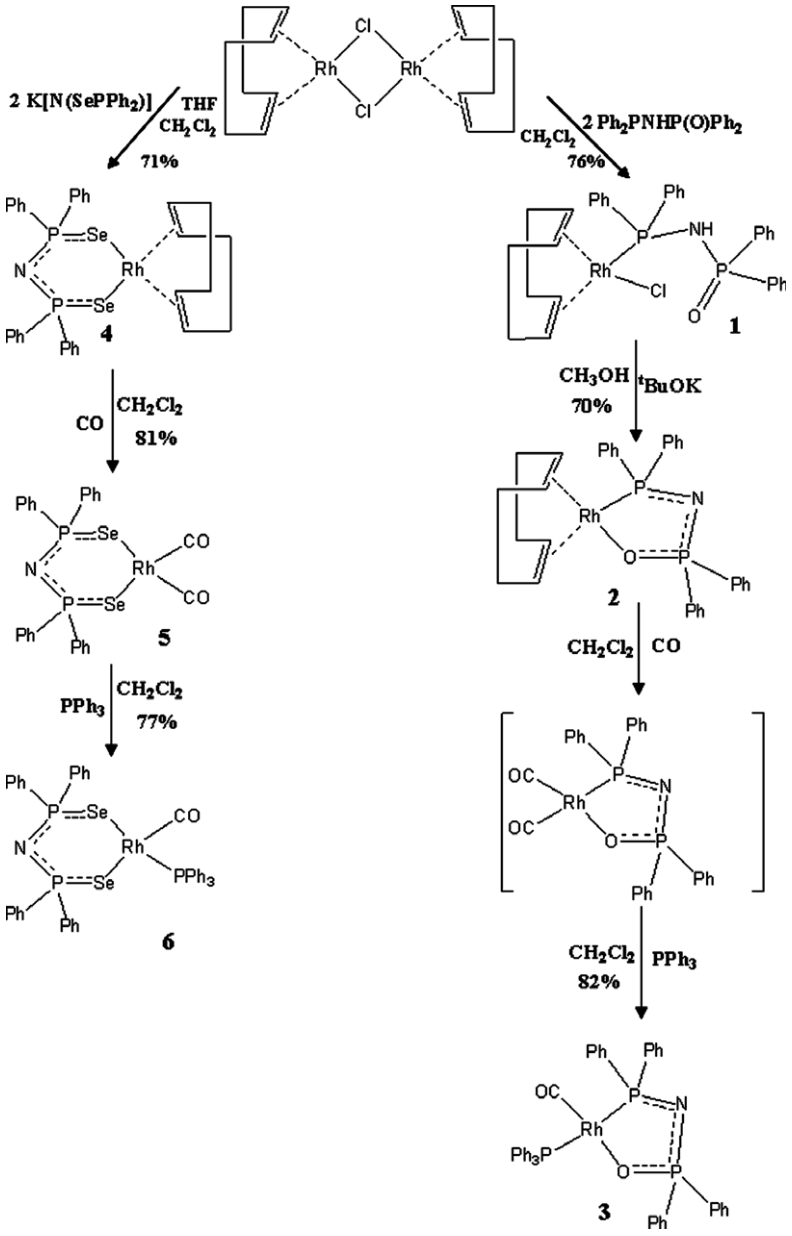

Scheme 1. Synthetic pathway for the preparation of complexes **3** and **6**.

assigned on the basis of published NMR data for **2** [23]. Finally, the high-field multiplet ($\delta_P = 30.1$, ddd) is assigned to $\mathbf{P}Ph_3$($^1J_{RhP} = 123.8$ Hz). Regarding the ^{1}H NMR spectrum of complex **3**, the phenyl protons of the *P*,*O*-ligand are observed in the aromatic region of the spectrum, between 7.6 (*ortho*, *para*) and 8.2 ppm (*meta*).

2.1.2. Rh^I complexes with the Se,Se-ligand

The ligand $[Ph_2P(Se)NP(Se)Ph_2]^-$ has already been employed to synthesize numerous complexes with several transition metals [34]. The synthesis of the complex [Rh(cod){$Ph_2P(Se)NP(Se)Ph_2$-*Se*,*Se*′}] (**4**) has been reported by Bhattacharyya et al. [24]. The (cod) ligand is

Table 2
Characteristic IR bands of the complexes containing the *P*,*O*-ligand

Complex	*ν*(CO)	*ν*(PNP)	*ν*(PO)	*ν*(NH)	*ν*(CH)
RhCl(cod){$Ph_2PNHP(O)Ph_2$-*P*} (**1**)	–	931	1220	3183	2981–3064
Rh(cod){$Ph_2PNP(O)Ph_2$-*P*,*O*} (**2**)	–	1101	1124	–	2824–3059
$Rh(CO)_2${$Ph_2PNP(O)Ph_2$-*P*,*O*}[a]	2084, 1992				
Rh(CO)(PPh_3){$Ph_2PNP(O)Ph_2$-*P*,*O*} (**3**)	1964	1103	1125	–	–

[a] Data in a CH_2Cl_2 solution.

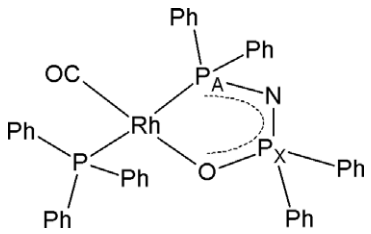

Fig. 1. P atom labeling used for the NMR spectrum of complex **3**.

replaced by two CO ligands upon treatment of **4** with an excess of CO, affording complex [Rh(CO)$_2${Ph$_2$P(Se)NP(Se)Ph$_2$-*Se*,*Se*′}] (**5**) (Scheme 1). Complex **5** shows, as expected, two terminal ν(CO) bands at 1981 cm^{-1} and 2046 cm^{-1} and no (cod) bands. Reaction of **5** with an equimolar quantity of PPh$_3$ yields the orange-yellow complex [Rh(CO)(PPh$_3$){Ph$_2$P(Se)NP(Se)Ph$_2$-*Se*,*Se*′}] (**6**) (Scheme 1). The IR spectrum of **6** shows a single terminal ν(CO) band at 1962 cm^{-1}, that is again indicative (vide supra) of an electron rich Rh^{I} centre. The shift of the ν(CO) band of **6** to lower frequencies, compared to **5**, suggests a reduction of the C–O bond order due to stronger π-back-bonding to the single remaining CO group. The ν(PSe) bands for complexes **5** and **6** appear at 541 cm^{-1} and 544 cm^{-1}, respectively.

The sequence of reactions can be followed *via* the changes in the characteristic IR bands of **4**, **5** and **6** presented in Table 3. In particular, the ν(CH) bands of the (cod) ligand in **4** disappear, while two new ν(CO) bands appear in the metal–carbonyl region of the IR spectrum of **5**. Finally, the replacement of one CO ligand by PPh$_3$ results in one single ν(CO) band in **6**.

The ^{31}P–{^{1}H} NMR spectrum of **6** could only be resolved at lower temperatures in toluene-d_8 (Figs. 3, S4 and S5). More specifically, only at −60 °C, the multiplets corresponding to the *Se*,*Se*-chelating ligand are clearly resolved, including the satellites resulting from coupling to ^{77}Se. The two P atoms of the *Se*,*Se*-chelate are no longer equivalent, due to the different ligands *trans* to each Se atom. Therefore, complex **6** as a whole, including the NMR active ^{103}Rh atom, can be best described as an ABMX spin-system (Fig. 4). The P atom of the phosphine ligand (**P$_X$**) is directly coordinated to the metal centre, thus giving rise to a low-field ddd-peak ($\delta_P = 39.4$). Coupling with ^{103}Rh ($^{1}J_{RhX} = 160.2$ Hz) is similar to the values of other complexes bearing PPh$_3$ directly coordinated to Rh^{I} [12,27,28]. The two high-field peaks are assigned to the two P atoms of the chelate ligand. In agreement with the stronger π-acidity of CO compared to PPh$_3$ and the J(*trans*) > J(*cis*) trend described for complex **3**, the dd-peak at 27.4 ppm is assigned to the P$_B$ atom, located *trans* to CO ($^{3}J_{BX} = 8.4$ Hz). On the other hand, the P$_A$ atom, located *trans* to PPh$_3$ and hence *cis* to CO, is slightly less deshielded, giving rise to an up-field doublet ($\delta_P = 26.1$), but exhibits stronger coupling with P$_X$($^{3}J_{AX} = 29.1$ Hz). Line broadening prevented us from calculating J_{RhP}, for this nucleus, even when we recorded the spectrum at −80 °C. Likewise, coupling between **P$_A$** and **P$_B$** was not resolved, as was also the case in the [Pd{Ph$_2$PNP(Se)Ph$_2$-*P*,*Se*}{N(SePPh$_2$)$_2$-*Se*,*Se*′}] complex, bearing the same *Se*,*Se*-ligand [24]. However, the ^{77}Se-satellites are observed for both nuclei, exhibiting typical coupling constants ($^{1}J_{PSe} = 550$ Hz and 552 Hz for P$_A$ and P$_B$, respectively) [24,34]. Furthermore, they provide strong evidence in favour of assigning the down-field peaks to the P atoms of the bidentate and not the phosphine ligand. It has to be noted that in a recent report on the synthesis of **6**, following a different synthetic procedure, the peak assignment was the opposite of the one presented here [35].

2.2. Single-crystal X-ray studies of complexes *3* and *6*

Suitable crystals of complexes **3** and **6** were grown by slow diffusion of *n*-hexane into a dichloromethane solution of each complex. The crystal structures of both complexes (Figs. 5, 6) were determined by single-crystal X-ray diffraction studies, and support the spectroscopic observations described above. Crystallographic data and refinement

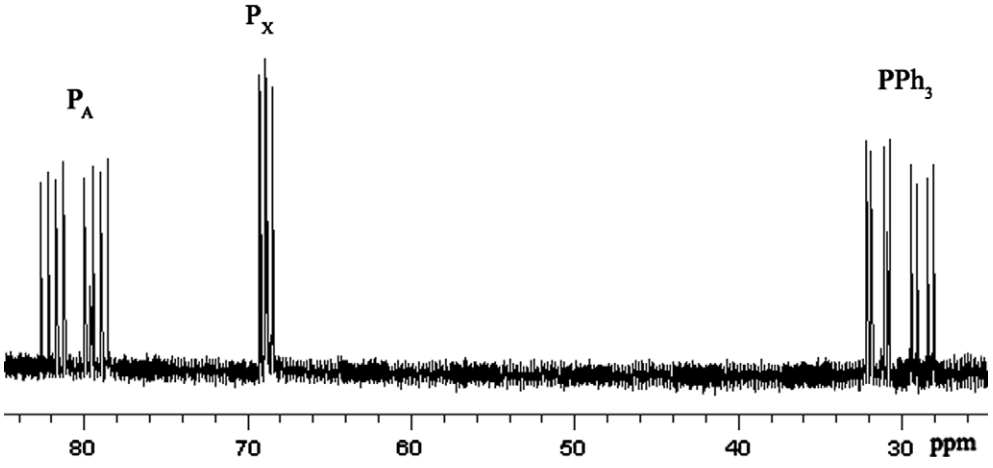

Fig. 2. The ^{31}P–{^{1}H} NMR spectrum of complex **3**.

Table 3
Characteristic IR bands of the complexes containing the *Se*,*Se*-ligand

Complex	*ν*(CO)	*ν*(PNP)	*ν*(PSe)	*ν*(CH)
[Rh(cod){$Ph_2P(Se)NP(Se)Ph_2$-*Se*,*Se*′}] (**4**)	–	1165	543	2821–3059
[$Rh(CO)_2${$Ph_2P(Se)NP(Se)Ph_2$-*Se*,*Se*′}] (**5**)	2046, 1981	1172	541	–
[Rh(CO)(PPh_3){$Ph_2P(Se)NP(Se)Ph_2$-*Se*,*Se*′}] (**6**)	1962	1168	544	–

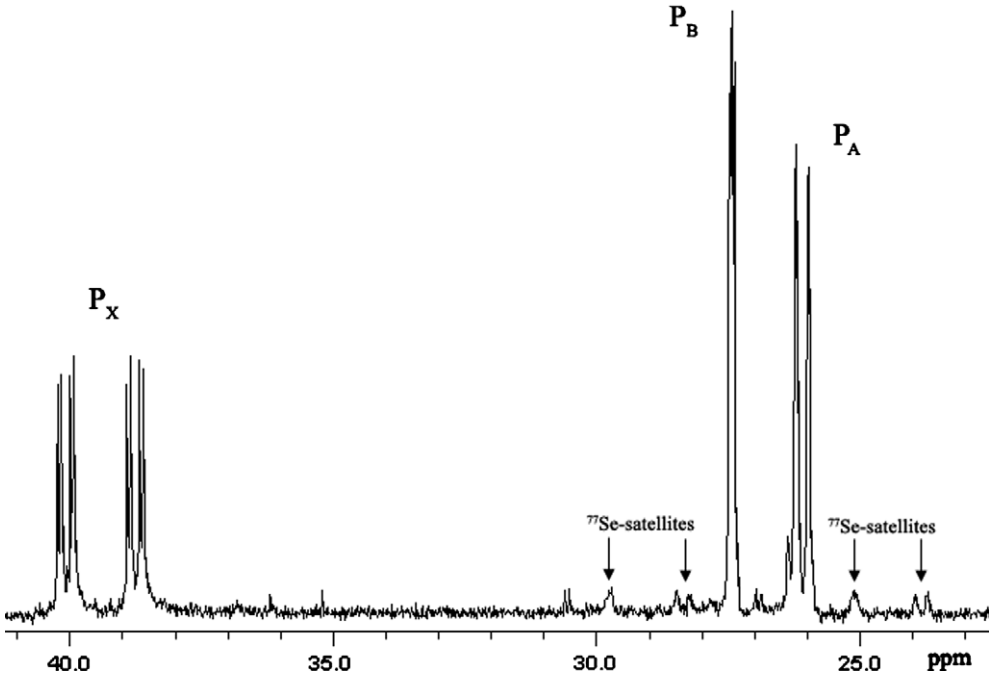

Fig. 3. The ^{31}P–{^{1}H} NMR spectrum of complex **6** at −60 °C.

parameters for both complexes are shown in Table 4, while the most characteristic bond lengths and angles of complexes **3** and **6** are listed in Tables 5 and 6, respectively.

The structure of complex **3** reveals a square-planar Rh^{I} centre coordinated by two P atoms at *trans* positions, one O atom and one CO group. The coordination of PPh_3 is *trans* to the P-atom of the bidentate *P*,*O*-ligand, due to the stronger *trans effect* of the P-atom, compared to the one of the O-atom, during the synthesis of **3** starting from the [$Rh(CO)_2${$Ph_2PNP(O)Ph_2$-*P*,*O*}] complex [12]. The five-membered Rh–P–N–P–O ring is slightly distorted from planar, in which, among the ring atoms, the N atom shows the biggest deviation (0.09 Å) from the Rh–O–P–N–P mean plane. The bond lengths in the chelate ring fall between those of typical single and double bonds, due to the delocalization of π-electron density along the ring, as has already been postulated by structural data [36,37] and theoretical calculations [38]. Furthermore, the C–O bond length of 1.165 Å is slightly bigger compared to similar Rh^{I}–carbonyl complexes (1.12–1.15 Å) [14,39,40], indi-

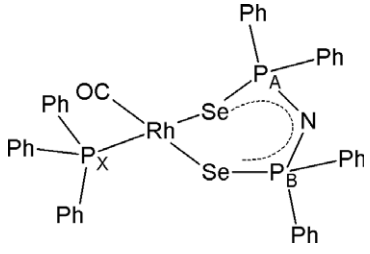

Fig. 4. P atom labeling used for the NMR spectrum of complex **6**.

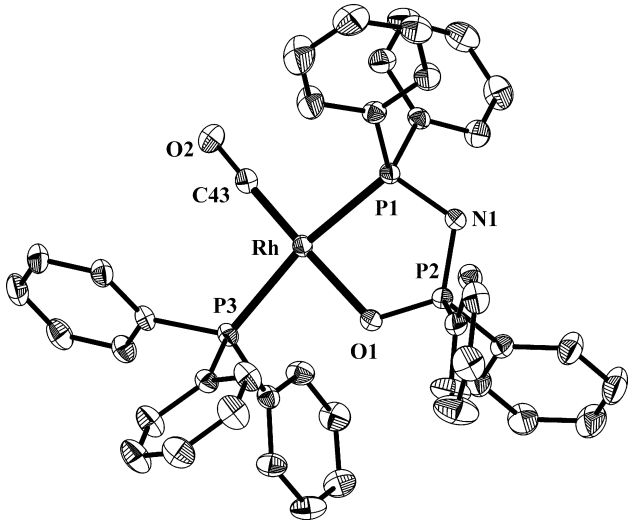

Fig. 5. Partially labeled ORTEP plot of **3** with ellipsoids drawn at the 30% probability level. Hydrogen atoms have been omitted for clarity.

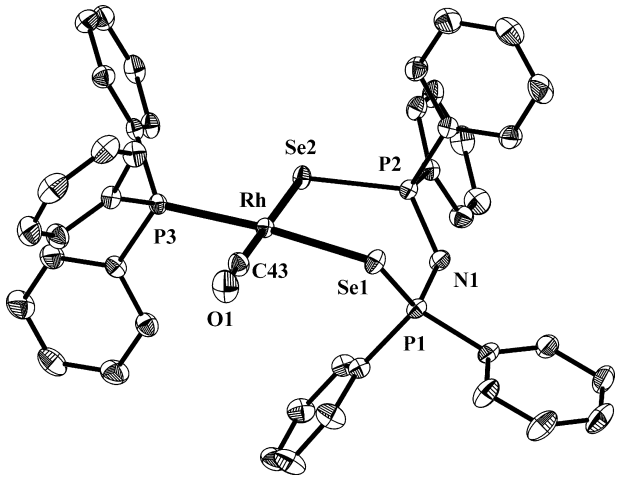

Fig. 6. Partially labeled ORTEP plot of **6** with ellipsoids drawn at the 30% probability level. Hydrogen atoms have been omitted for clarity.

cating high electron density at the Rh^I centre and stronger π-back-bonding. This observation verifies the analysis based on the IR spectrum of complex **3**, in which the low *ν*(CO) band would imply an electron rich metal centre.

The core of complex **6**, RhSeSeP(CO), adopts a square-planar geometry around the metal centre. The six-membered Rh–Se–P–N–P–Se ring is not planar, since atoms P(1) and N(1) are displaced 1.54 Å and 1.14 Å, respectively, out of the mean plane of the remaining four atoms, resulting in a slightly distorted boat ring conformation, with Se(1) and P(2) located at the apices.

In analogy to complex **3**, the bond lengths along the Rh–Se–P–N–P–Se ring fall between those of typical single and double bonds due to the delocalization of π-electron density along the chelate ring [36–38]. The bond length difference between the Rh–Se(1) and Rh–Se(2) bonds (2.516 Å and 2.506 Å, respectively), is due to the stronger *trans influence* of the PPh_3 ligand compared to CO. Similar observations have been made in analogous systems, such as [Pd{$Ph_2PNP(Se)Ph_2$-*P*,*Se*}{$N(SePPh_2)_2$-*Se*,*Se*′}] [24], [$PtCl_2${$PPh_2N(Ph)P(S)Ph_2$-*P*,*S*}] [33] and [Rh(CO)(PPh_3)-{$Ph_2P(S)NP(S)Ph_2$-*S*,*S*′}] [41].

Furthermore, as in the case of complex **3**, the C–O bond length, at 1.147 Å, is larger than in other Rh^I–carbonyl complexes [14,39,40], indicating high electron density at the Rh^I centre which, through strong π-back donation, weakens the carbonyl C–O bond. This observation is also in agreement with the IR spectroscopic data of complex **6** presented above.

The bond length of the Rh–PPh_3 bond in complex **3** is larger by 0.015 Å compared to complex **6**, possibly due to the stronger *trans influence* exerted by the Rh-coordinated P atom of the *P*,*O*-ligand, compared to the Se atom of the *Se*,*Se*-ligand, respectively. This difference might explain the smaller ^1J(Rh–PPh_3) in the case of **3** (123.8 Hz) compared to **6** (160.2 Hz) (vide supra).

Table 4
Crystal data and structure refinement details for complexes **3** and **6**

Compound	**3**	**6**
Empirical formula	$C_{43}H_{35}NO_2P_3Rh$	$C_{43}H_{35}NOP_3RhSe_2$
Formula weight	793.54	935.46
Temperature (K)	298	298
Space group	$P\bar{1}$	$P\bar{1}$
Unit cell dimensions		
a (Å)	10.785(5)	9.791(2)
b (Å)	18.937(9)	11.971(3)
c (Å)	9.525(5)	18.390(4)
α (°)	93.86(2)	107.43(1)
β (°)	95.49(2)	98.14(1)
γ (°)	97.48(2)	101.30(1)
Volume (Å^3)	1913.7(16)	1969.9(8)
Z	2	2
ρ_{calc} (Mg m^{-3})	1.377	1.577
μ (mm^{-1})	5.080	2.438
R_1^a	0.0361[b]	0.0409[c]
wR_2^a	0.0963[b]	0.1021[c]

[a] $w = 1/[\sigma^2(F_o^2) + (aP)^2 + bP]$ and $P = \max(F_o^2,0) + (2F_c^2)/3$; $R_1 = \sum(|F_o| - |F_c|)/\sum(|F_o|)$ and $wR_2 = \{\sum[w(F_o^2 - F_c^2)^2]/\sum[w(F_o^2)^2]\}^{1/2}$.
[b] For 4928 reflections with $I > 2\sigma(I)$.
[c] For 5833 reflections with $I > 2\sigma(I)$.

Table 5
Selected bond lengths and angles for complex **3**

Bond lengths (Å)		Bond angles (°)	
Rh–P(1)	2.271(1)	C(43)–Rh–O(1)	177.0(1)
Rh–P(3)	2.294(1)	C(43)–Rh–P(1)	94.7(1)
Rh–O(1)	2.092(3)	O(1)–Rh–P(1)	83.7(1)
Rh–C(43)	1.801(4)	C(43)–Rh–P(3)	96.0(1)
P(1)–N(1)	1.637(3)	O(1)–Rh–P(3)	85.6(1)
P(2)–O(1)	1.517(3)	P(1)–Rh–P(3)	169.4(1)
P(2)–N(1)	1.576(3)	N(1)–P(1)–Rh	107.4(1)
C(43)–O(2)	1.165(5)	O(1)–P(2)–N(1)	113.6(2)
		P(2)–O(1)–Rh	118.5(1)
		P(2)–N(1)–P(1)	116.3(2)
		O(2)–C(43)–Rh	178.1(4)

Table 6
Selected bond lengths and angles for complex **6**

Bond lengths (Å)		Bond angles (°)	
Rh–Se(1)	2.516(1)	C(43)–Rh–P(3)	88.9(1)
Rh–Se(2)	2.506(1)	C(43)–Rh–Se(2)	179.7(1)
Rh–P(3)	2.279(1)	P(3)–Rh–Se(2)	91.4(1)
Rh–C(43)	1.816(5)	C(43)–Rh–Se(1)	80.8(1)
Se(1)–P(1)	2.170(1)	P(3)–Rh–Se(1)	169.7(1)
Se(2)–P(2)	2.191(1)	Se(2)–Rh–Se(1)	98.9(1)
C(43)–O(1)	1.146(6)	P(1)–Se(1)–Rh	100.2(1)
P(1)–N(1)	1.591(4)	P(2)–Se(2)–Rh	107.6(1)
P(2)–N(1)	1.600(3)	O(1)–C(43)–Rh	176.1(1)
		N(1)–P(1)–Se(1)	115.9(1)
		N(1)–P(2)–Se(2)	119.02(1)
		P(1)–N(1)–P(2)	124.2(1)

2.3. Catalytic activity of complexes 2, 3 and 6 towards hydroformylation of styrene

The complexes **2** and **3** were studied as catalysts in the hydroformylation of styrene (**7**) under variable conditions

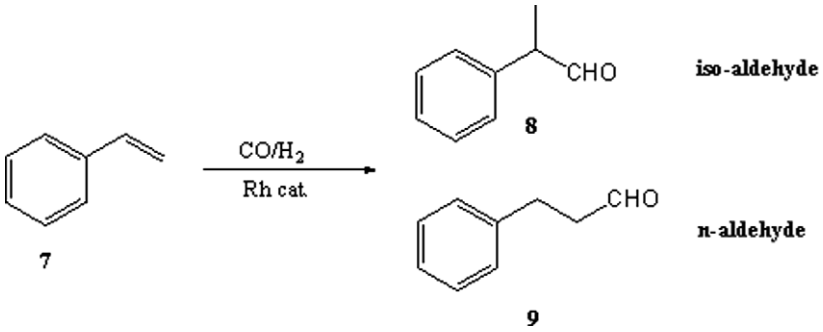

Scheme 2. Hydroformylation of styrene.

Table 7
Hydroformylation of styrene catalyzed by complexes **2** and **3**[a]

Entry	Complex	P[b] (bar)	T (°C)	Time (h)	Conversion (%)	R_c[c] (%)	R_{br}[d] (%)	TON[e]
1	**2**	100	60	2	78.6	97.1	89.8	1110
2	**3**	100	60	2	96.1	99.5	93.6	1391
3	**2**	100	30	20	88.2	99.3	98.3	1274
4	**3**	100	40	4	31.3	99.1	96.6	451
5	**2**	50	60	2	72.3	100.0	83.3	1052
6	**2**	30	60	20	87.7	97.7	77.1	1247
7	**3**	30	60	20	99.8	99.4	85.6	1443
8	**3**	30	40	20	49.3	98.7	92.4	708
9	**3**	10	40	72	40.8	98.5	75.5	585

[a] A 4 mM solution in CH_2Cl_2. Styrene:catalyst = 1455:1.
[b] P = initial total pressure of CO/H_2 (1/1).
[c] R_c = chemoselectivity for aldehydes.
[d] R_{br} = regioselectivity towards branched aldehyde.
[e] Turnover number (TON) = aldehydes fraction × substrate:[Rh] ratio.

of pressure and temperature (Scheme 2, Table 7). The catalytic experiments were performed in an autoclave, by mixing styrene and a stock solution of the rhodium complex (4 mM in CH_2Cl_2) with a molar ratio styrene/catalyst of 1455:1, using syngas CO/H_2 (1:1). Complexes **2** and **3** displayed good activity, high chemoselectivity for aldehydes (97–100%), and high regioselectivity for the formation of the branched aldehyde of up to 98%. The variation observed in this work in the conversions of styrene and the regioselectivities in the resulting branched aldehyde, under variable conditions of pressure and temperature, was as expected for hydroformylation of styrene using rhodium systems, that is, an increased temperature speeds up the catalytic reaction, but at the same time decreases the regioselectivity, and an increased pressure increases both the reaction rate and the regioselectivity. The results were acceptable even at the low pressures of 30 or 10 bar (entries 6–9). Complex **3** bearing one more phosphorus donor compared to complex **2** displayed higher reaction rates and selectivities than **2** (compare entries 1–2 and 6–7). The good activity of complexes **2** and **3** could partly be attributed to free coordination sites that would be easily formed in both complexes during the course of the catalytic reaction. The (cod) ligand of complex **2** would be easily removed, while the strong *trans effect* of CO could weaken the Rh–O bond in complex **3**, opening the five-membered chelate ring. Similar hemilabile behavior of phosphorous chelate ligands has been considered as beneficial for hydroformylation reactions [42]. The PPh_3 group in complex **3** could also be served for an additional stabililization of the active species during the course of the metal-mediated reaction.

On the other hand, complex **6** in which rhodium is bound to a CO, PPh_3 and a *Se*,*Se*-ligand forming a six-membered chelate ring, showed none or very low catalytic activity, for reasons being still unclear. Perhaps, this is due to the saturated coordinated-rhodium atom, being unable to obtain free coordination sites and to proceed the catalytic cycle.

3. Conclusions

In summary, complexes containing electron rich Rh^I centres and bearing (cod), CO, PPh_3 and *P*,*O*- or *Se*,*Se*-ligands have been synthesized, structurally and spectroscopically characterized, and applied as catalysts for the hydroformylation of styrene. The IR and NMR spectra have been thoroughly analyzed, and compared with similar systems in the literature. In the structures of complexes **3** and **6**, different *trans influence* effects of the ligands are clearly manifested. The complexes **2** and **3**, which contain the *P*,*O*-ligand forming a five-membered ring with Rh, exhibit the best catalytic activity for the hydroformylation of styrene.

4. Experimental

4.1. General procedures

Unless otherwise stated, all manipulations were carried out under an inert Ar atmosphere, using pre-dried solvents and standard Schlenk techniques.[RhCl(cod){Ph_2-PNHP(O)Ph_2-*P*}] (**1**), [Rh(cod){Ph_2PNP(O)Ph_2-*P*,*O*}] (**2**) and [Rh(cod){Ph_2P(Se)NP(Se)Ph_2-*Se*,*Se*′}] (**4**) were prepared from $[RhCl(cod_2)]_2$ (Aldrich) and the appropriate diphosphine ligands, according to reported procedures [23,24]. All the other chemicals were commercially available. Hydroformylation using syngas (CO–H_2, 1:1) was performed in a stainless steel autoclave (300 mL) with magnetic stirring. Elemental analyses (C, H and N) were performed in a Perkin–Elmer PE 2400II, CHNS/O analyzer. Infrared spectra were recorded between 4000 and 200 cm^{-1} on a Perkin–Elmer 833 spectrometer. NMR spectra were recorded in a Varian Unity Plus spectrometer. TMS (^{1}H NMR) and 85% H_3PO_4 in D_2O (^{31}P NMR) were used as reference. The products of the catalytic reactions were detected and quantified by Gas Chromatography (Varian Star 3400 CX with a 30 m × 0.53 mm DB5 column).

4.2. [Rh(CO)(PPh_3){Ph_2PNP(O)Ph_2-*P*,*O*}] (**3**)

[Rh(cod){Ph_2PNHP(O)Ph_2-*P*,*O*}] (0.128 g, 0.209 mmol) was dissolved in toluene (25 mL) and the solution was subjected to CO bubbling for 20 min, during which the colour rapidly turned from yellow to orange, indicating the generation of the dicarbonyl intermediate. At this point, an equivalent amount of PPh_3 was added (0.058 g, 0.221 mmol), changing the colour of the solution to pale-yellow. The reaction mixture was stirred for 1.5 h at room temperature, and, subsequently, it was concentrated under reduced pressure up to 2–3 mL. Addition of *n*-hexane (30 mL) afforded the yellow solid compound, [Rh(CO)-(PPh_3){Ph_2PNHP(O)Ph_2-*P*,*O*}], which was collected by filtration, washed with 10 mL of *n*-hexane and finally dried *in vacuo*. Yield: 0.202 g (82%). Anal. Calc. for $C_{43}H_{35}NO_2P_3Rh$: C, 65.09; H, 4.45; N, 1.77. Found: C, 65.88; H, 4.58; N, 1.84%. Selected IR data (KBr, cm^{-1}): 1964 [*ν*(CO)], 1125 [*ν*(PO)], 1103 [*ν*(PNP)]. ^{1}H NMR (300 MHz, toluene-d_8):δ_H 8.13 (m, 14H, *m*-C_6H_5), 7.67 (m, 21H, *o*,*p*-C_6H_5). ^{31}P–{^{1}H} NMR (121.5 MHz, toluene-d_8): δ_P 80.6 [ddd, P_A, $^2J(P_APPh_3) = 327.5$ Hz, $^1J(RhP_A) = 119.0$ Hz, $^2J(P_AP_X) = 52.8$ Hz], 68.9 [ddd, P_X, $^2J(P_AP_X) = 52.8$ Hz, $^3J(P_XPPh_3) = 41.3$ Hz, $^2J(RhP_X) = 3.7$ Hz], 30.1 [ddd, PPh_3, $^2J(P_APPh_3) = 327.5$ Hz, $^1J(RhPPh_3) = 123.8$ Hz, $^3J(P_XPPh_3) = 41.3$ Hz].

4.3. [Rh(CO)$_2${Ph_2P(Se)NP(Se)Ph_2-*Se*,*Se*′}] (**5**)

[Rh(cod){Ph_2P(Se)NP(Se)Ph_2-*Se*,*Se*′}] (0.070 g, 0.092 mmol) was dissolved in CH_2Cl_2 (15 mL), and the solution was subjected to CO bubbling for 20 min, during which the colour turned from orange to yellow-green. The volume of the reaction mixture was reduced to 2–3 mL and addition of *n*-hexane (30 mL) afforded an orange solid which was filtered *in vacuo* and washed with small portions of *n*-hexane. Yield: 0.053 g (81%). Selected IR data (KBr, cm^{-1}): 2046 [ν_{as}(CO)], 1981 [ν_{sym}(CO)], 1172 [*ν*(PNP)], 541 [*ν*(PSe)].

4.4. [Rh(CO)(PPh_3){Ph_2P(Se)NP(Se)Ph_2-*Se*,*Se*′}] (**6**)

[Rh(cod){Ph_2P(Se)NP(Se)Ph_2-*Se*,*Se*′}] (0.050 g, 0.065 mmol) was dissolved in 20 mL of toluene and the solution was subjected to CO bubbling for 20 min, during which the colour turned from orange to yellow-green. At this point, an equivalent amount of PPh_3 was added (0.020 g, 0.070 mmol), changing the colour of the solution to pale-yellow. The reaction mixture was stirred for 1.5 h at room temperature and, subsequently, it was concentrated under reduced pressure up to 2–3 mL. Addition of *n*-hexane (20 mL) afforded the orange solid compound [Rh(CO)(PPh_3){Ph_2P(Se)NP(Se)Ph_2-*Se*,*Se*′}], which was collected by filtration, washed with small portions of *n*-hexane and finally dried *in vacuo*. Yield: 0.055 g (77%). Anal. Calc. for $C_{43}H_{35}NOP_3RhSe_2$: C, 57.07; H, 4.28; N, 1.86. Found: C, 51.02; H, 2.61; N, 1.73%. Selected IR data (KBr, cm^{-1}): 1962 [*ν*(CO)], 1168 [*ν*(PNP)], 544 [*ν*(PSe)]. ^{1}H NMR (300 MHz, toluene-d_8): δ_H 8.36 (m, 14H, *m*-C_6H_5), 7.74 (m, 21H, *o*,*p*-C_6H_5). ^{31}P–{^{1}H} NMR (121.5 MHz, toluene-d_8): δ_P 39.4 [ddd, P_X, $^1J(RhP_X) = 160.2$ Hz, $^3J(P_AP_X) = 29.1$ Hz, $^3J(P_BP_X) = 8.4$ Hz], 27.4 [dd, P_B, $^3J(P_BP_X) = 8.4$ Hz, $^2J(RhP_B) = 3.9$ Hz, $^1J(P_BSe) = 552$ Hz, satellites], 26.1 [d, P_A, $^3J(P_AP_X) = 29.1$ Hz, $^1J(P_ASe) = 550$ Hz, satellites].

4.5. Hydroformylation of styrene

In a typical experiment, styrene (2 mL, 17.456 mmol), a 4 mM solution of rhodium complex in dichloromethane (3 mL, 0.012 mmol) were placed under argon in an oven-dried autoclave, which was then closed, pressurized with syngas (CO–H_2, 1:1) to the appropriate pressure and brought to the required temperature. After the required reaction time, the autoclave was cooled to room temperature, the pressure was carefully released, the solution was diluted with dichloromethane, passed through celite and analyzed by GC. Conversions were determined by GC.

4.6. X-ray crystallography

A light yellow prismatic crystal of **3** (0.10 × 0.25 × 0.35 mm) was mounted in capillary and a yellow prismatic crystal of **6** (0.20 × 0.30 × 0.75 mm) was mounted in air and covered with epoxy glue. Diffraction measurements were made on a $P2_1$ Nicolet diffractometer upgraded by Crystal Logic for **3** using graphite-monochromated Cu radiation, and on a Crystal Logic Dual Goniometer diffractometer for **6** using graphite-monochromated Mo radiation.

Important crystal data and parameters for data collection are reported in Table 4. Unit cell dimensions were determined and refined by using the angular settings of 25 automatically centred reflections in the range $22° < 2\theta < 54°$ for **3** and $11° < 2\theta < 23°$ for **6**. Three standard reflections monitored every 97 reflections showed less than 3% intensity fluctuation and no decay. Lorentz polarization and ψ-scan absorption corrections were applied using Crystal Logic software. The structures were solved by direct methods using SHELXS-86 [43] and refined by full-matrix least-square on F^2 using SHELXL-97 [44]. Further experimental crystallographic details for **3**: $2\theta_{max} = 120°$, scan speed 4.5°/min; scan range $2.45 + \alpha_1\alpha_2$ separation; reflections collected/unique/used, 5678/5341 [$R_{int} = 0.0279$]/5341; 592 parameters refined; $(\Delta/\sigma)_{max} = 0.006$;$(\Delta\rho)_{max}/(\Delta\rho)_{min} = 0.510/-0.794$ e/Å^3; R/R_w (for all data), 0.0397/0.1000. All hydrogen atoms were located by difference maps and were refined isotropically. All non-H atoms were refined anisotropically. Further experimental crystallographic details for **6**: $2\theta_{max} = 50°$, scan speed 2.2°/min; scan range $1.6 + \alpha_1\alpha_2$ separation; reflections collected/unique/used, 7386/6946 [$R_{int} = 0.0161$]/6946; 600 parameters refined; $(\Delta/\sigma)_{max} = 0.003$; $(\Delta\rho)_{max}/(\Delta\rho)_{min} = 1.431/-0.670$ e/Å^3; R/R_w (for all data), 0.0526/0.1104. All hydrogen atoms were located by difference maps and were refined isotropically. All non-H atoms were refined anisotropically.

Acknowledgements

The project is co-funded by the European Social Fund and National Resources – (EPEAEK II) PYTHAGORAS. The Special Research Account of NKUA, the EPEAEK program "Catalysis and its Applications", and the General Secretariat of Research and Technology of Greece are also acknowledged.

Appendix A. Supplementary material

CCDC 645202 and 645203 contain the supplementary crystallographic data for **3** and **6**. These data can be obtained free of charge via http://www.ccdc.cam.ac.uk/conts/retrieving.html, or from the Cambridge Crystallographic Data Centre, 12 Union Road, Cambridge CB2 1EZ, UK; fax: (+44) 1223-336-033; or e-mail: deposit@ccdc.cam.ac.uk. Supplementary data associated with this article can be found, in the online version, at doi:10.1016/j.jorganchem.2007.06.032.

References

[1] P.W.N.M. Van Leeuwen, C. Claver, Rhodium Catalyzed Hydroformylation, Kluwer Academic Publishers, Dordrecht, 2000.
[2] A.M. Trzeciak, J.J. Ziolkowski, Coord. Chem. Rev. 192 (1999) 883–900.
[3] C.M. Thomas, G. Suss-Fink, Coord. Chem. Rev. 243 (2003) 125–142.
[4] B. Cornils, W.A. Herrmann, Applied Homogeneous Catalysis with Organometallic Compounds: A Comprehensive Handbook in Three Volumes, second ed., Wiley–VCH, Weinheim, 2002.
[5] C.S. Slone, D.A. Weinberger, C.A. Mirkin, in: K.D. Karlin (Ed.), Progress in Inorganic Chemistry, Wiley, New York, 1999, pp. 233–350.
[6] P. Braunstein, F. Naud, Angew. Chem., Int. Ed. 40 (2001) 680–699.
[7] R.W. Wegman, A.G. Abatjoglou, A.M. Harrison, J. Chem. Soc., Chem. Commun. (1987) 1891–1892.
[8] M.J. Baker, M.F. Giles, A.G. Orpen, M.J. Taylor, R.J. Watt, J. Chem. Soc., Chem. Commun. (1995) 197–198.
[9] D.K. Dutta, J.D. Woollins, A.M.Z. Slawin, D. Konwar, P. Das, M. Sharma, P. Bhattacharyya, S.M. Aucott, Dalton Trans. (2003) 2674–2679.
[10] D.K. Dutta, J.D. Woollins, A.M.Z. Slawin, D. Konwar, M. Sharma, P. Bhattacharyya, S.M. Aucott, J. Organomet. Chem. 691 (2006) 1229–1234.
[11] P. Chutia, B.J. Sarmah, D.K. Dutta, Appl. Organomet. Chem. 20 (2006) 512–520.
[12] P. Braunstein, Y. Chauvin, J. Nahring, A. DeCian, J. Fischer, A. Tiripicchio, F. Ugozzoli, Organometallics 15 (1996) 5551–5567.
[13] A.M. Trzeciak, J.J. Ziolkowski, T. Lis, R. Choukroun, J. Organomet. Chem. 575 (1999) 87–97.
[14] P. Stepnicka, I. Cisarova, J. Chem. Soc., Dalton Trans. (1998) 2807–2811.
[15] A.M. Trzeciak, P. Stepnicka, E. Mieczynska, J.J. Ziolkowski, J. Organomet. Chem. 690 (2005) 3260–3267.
[16] E.I. Tolis, K.A. Vallianatou, F.J. Andreadaki, I.D. Kostas, Appl. Organomet. Chem. 20 (2006) 335–337.
[17] I.D. Kostas, K.A. Vallianatou, J. Holz, A. Borner, Appl. Organomet. Chem. 19 (2005) 1090–1095.
[18] I.D. Kostas, B.R. Steele, F.J. Andreadaki, V.A. Potapov, Inorg. Chim. Acta 357 (2004) 2850–2854.
[19] I.D. Kostas, C.G. Screttas, J. Organomet. Chem. 585 (1999) 1–6.
[20] I.D. Kostas, Inorg. Chim. Acta 355 (2003) 424–427.
[21] I.D. Kostas, J. Organomet. Chem. 634 (2001) 90–98.
[22] I.D. Kostas, J. Organomet. Chem. 626 (2001) 221–226.
[23] A.M.Z. Slawin, M.B. Smith, J.D. Woollins, J. Chem. Soc., Dalton Trans. (1996) 1283–1293.
[24] P. Bhattacharyya, A.M.Z. Slawin, D.J. Williams, J.D. Woollins, J. Chem. Soc., Dalton Trans. (1995) 2489–2495.
[25] J. Rankin, A.D. Poole, A.C. Benyei, D.J. Cole-Hamilton, J. Chem. Soc., Chem. Commun. (1997) 1835–1836.
[26] A.M. Trzeciak, B. Borak, Z. Ciunik, J.J. Ziolkowski, M.F.C.G. da Silva, A.J.L. Pombeiro, Eur. J. Inorg. Chem. (2004) 1411–1419.
[27] L. Dahlenburg, K. Herbst, M. Kuhnlein, Z. Anorg. Allg. Chem. 623 (1997) 250–258.
[28] M. Lamac, I. Cisarova, P. Stepnicka, J. Organomet. Chem. 690 (2005) 4285–4301.
[29] I.J. Colquhoun, W. McFarlane, J. Chem. Soc., Dalton Trans. (1977) 1674–1679.
[30] A. Bright, B.E. Mann, C. Masters, B.L. Shaw, R.M. Slade, R.E. Stainbank, J. Chem. Soc. (A) (1971) 1826–1831.
[31] P. Braunstein, Y. Chauvin, J. Fischer, H. Olivier, C. Strohmann, D.V. Toronto, New J. Chem. 24 (2000) 437–445.
[32] A.M.Z. Slawin, M.B. Smith, J.D. Woollins, J. Chem. Soc., Dalton Trans. (1996) 4575–4581.
[33] M.S. Balakrishna, R. Klein, S. Uhlenbrock, A.A. Pinkerton, R.G. Cavell, Inorg. Chem. 32 (1993) 5676–5681.
[34] L. Marquez-Pallares, J. Pluma-Pluma, M. Reyes-Lezama, M. Guizado-Rodriguez, H. Hopfl, N. Zuniga-Villareal, J. Organomet. Chem. 692 (2007) 1698–1707.
[35] W.M. Cheung, C.Y. Lai, Q.F. Zhang, W.Y. Wong, I.D. Williams, W.H. Leung, Inorg. Chim. Acta 359 (2006) 2712–2720.
[36] C. Silvestru, J.E. Drake, Coord. Chem. Rev. 223 (2001) 117–216.
[37] T.Q. Ly, J.D. Woollins, Coord. Chem. Rev. 176 (1998) 451–481.

[38] D. Maganas, S.S. Staniland, A. Grigoropoulos, F. White, S. Parsons, N. Robertson, P. Kyritsis, G. Pneumatikakis, Dalton Trans. (2006) 2301–2315.
[39] A.M. Trzeciak, T. Glowiak, R. Grzybek, J.J. Ziolkowski, J. Chem. Soc., Dalton Trans. (1997) 1831–1837.
[40] S. Burger, B. Therrien, G. Suss-Fink, Helv. Chim. Acta 88 (2005) 478–486.
[41] D. Symeonidis, M.Sc. Thesis, University of Athens, 2003.
[42] I. Le Gall, P. Laurent, E. Soulier, J.Y. Salaun, H. des Abbayes, J. Organomet. Chem. 567 (1998) 13–20.
[43] G.M. Sheldrick, SHELXS-86: Structure Solving Program, University of Göttingen, Göttingen, Germany, 1986.
[44] G.M. Sheldrick, SHELXL-97: Crystal Structure Refinement, University of Göttingen, Göttingen, Germany, 1997.